Scientific Research Publishing

Open Journal of Ecology, 2024, 14, 523-543
https://www.scirp.org/journal/oje
ISSN Online: 2162-1993
ISSN Print: 2162-1985

Analysis of the Spatiotemporal Variation Characteristics and Driving Factors of Land Vegetation GPP in a Certain Region of Asia

Zhongshuai Xia

School of Civil and Hydraulic Engineering, Qinghai University, Xining, China
Email: x779642583@163.com

How to cite this paper: Xia, Z.S. (2024) Analysis of the Spatiotemporal Variation Characteristics and Driving Factors of Land Vegetation GPP in a Certain Region of Asia. *Open Journal of Ecology*, **14**, 523-543.
https://doi.org/10.4236/oje.2024.146030

Received: May 3, 2024
Accepted: June 10, 2024
Published: June 13, 2024

Abstract

Gross primary productivity (GPP) of vegetation is a critical indicator of ecosystem growth and carbon sequestration. The spatiotemporal variation characteristics of land vegetation GPP trends in a specific region of Asia from 2001 to 2020 were analyzed by Sen and MK trend analysis methods in this study .Moreover , a GPP change attribution model was established to explore the driving influences of factors such as Leaf Area Index (LAI), Land Surface Temperature (LST), Vapor Pressure Deficit (VPD), Soil Moisture, Solar Radiation and Wind Speed on GPP. The results indicate that summer GPP values are significantly higher than those in other months, accounting for 60.8% of the annual total GPP; spring and autumn contribute 18.91% and 13.04%, respectively. In winter, due to vegetation being nearly dormant, the contribution is minimal at 7.19%. Spatially, GPP shows a decreasing trend from southeast to northwest. LAI primarily drives the spatial and seasonal variations of regional GPP, while VPD, surface temperature, solar radiation, and soil moisture have varying impacts on GPP across different dimensions. Additionally, wind speed exhibits a minor contribution to GPP across different dimensions.

Keywords

Gross Primary Productivity, Spatiotemporal Variations, Model, Driving Factors

1. Introduction

Terrestrial vegetation gross primary productivity (GPP) forms the foundation of energy flow within ecosystems. Through the process of photosynthesis, GPP converts solar energy into organic matter, sustaining the stability of food chains and food webs. It plays a crucial role in the carbon cycle and the regulation of

ecological processes. GPP serves as a significant indicator of carbon sequestration capability and the growth characteristics of terrestrial vegetation, providing a direct reflection of ecosystem health and productivity levels.

There exists a close relationship between GPP and the spatiotemporal variations of vegetation phenology. This relationship is regulated by various ecological and climatic factors [1] [2]. Vegetation phenology, which reflects the growth and development processes of plants, is significantly influenced by climate factors such as temperature, precipitation, and solar radiation. Changes in temperature and precipitation patterns induced by climate change can profoundly impact vegetation phenology, leading to extended or shortened growing seasons and altered growth stages [3]. Understanding the spatiotemporal evolution patterns of GPP is vital for regional sustainable development and ecological civilization construction [4].

Global changes, particularly marked by climate warming, have extensive and profound impacts on terrestrial ecosystems. The primary driver of climate warming is the increased emissions of greenhouse gases such as Carbon dioxide due to human activities [5]. The growth of terrestrial vegetation is closely linked to global climate changes [6]. Over the past few decades, the greening of the global surface has enhanced the carbon sink function of vegetation, slowing the rate of increase in global Carbon dioxide concentrations and playing a crucial role in climate regulation [7].

This study employed the Sen + MK trend analysis method to analyze the trends in GPP changes in a certain region of Asia from 2001 to 2020. A GPP change driving attribution model was established, using this model to explore the driving impacts of factors such as Leaf Area Index (LAI), Land Surface Temperature (LST), Saturation Vapor Pressure Deficit (SVPD), Soil Moisture, Solar Radiation and Wind Speed on GPP. The spatiotemporal variation characteristics of the terrestrial ecosystem's gross primary productivity in the study area were systematically analyzed, clarifying its intrinsic driving mechanisms. It is significant scientific implications for the formulation of ecological protection and restoration measures in the region.

2. Study Region Overview, Data Sources, and Methods

2.1. Study Region Overview

The study region is located in a specific region of Asia, covering approximately 395,000 square kilometers. Situated at an average elevation of over 4000 meters, the region is predominantly characterized by mountainous terrain. The region features complex topography, with widespread mountain ranges and rugged landscapes. Overall, the terrain gradually rises from the southeast to the northwest, forming a pronounced uplift trend.

2.2. Data Sources

2.2.1. Gross Primary Productivity (GPP_{SIF})

The GPP data used in this study is derived from the empirical relationship between GPP and SIF, resulting in a global GPP-SIF product at a spatial resolution

of 0.05˚ and a temporal resolution of 8 days for the years 2001-2020 [8].

2.2.2. Leaf Area Index (LAI)

Leaf Area Index (LAI) is a critical parameter describing the extent of vegetation canopy coverage. It represents the ratio of total leaf surface area to the ground area per unit area. Data for LAI are sourced from the Moderate Resolution Imaging Spectroradiometer (MODIS) Vegetation Indices product MOD15A2H, provided by the Land Processes Distributed Active Archive Center (LP DAAC), which is part of NASA's Earth Observing System (EOS).

2.2.3. Climatic Factors

Land Surface Temperature (LST) serves as a critical indicator of the interface between the Earth's surface and the atmosphere. It directly reflects the exchange of energy between the land surface and the atmosphere and plays a complex role in the land-atmosphere interaction processes. The LST data used in this study are derived from the TRIMS LST (Thermal and Reanalysis Integrating Moderate-resolution Spatial-seamless LST) dataset [9]. This dataset employs an enhanced satellite thermal infrared remote sensing-reanalysis data integration method to prepare LST data [9].

Wind speed is an important parameter for atmospheric motion and has significant implications for meteorological disaster prediction, wind energy utilization, ocean circulation, and other applications. It refers to the velocity of wind motion and is typically expressed in meters per second (m/s) or other appropriate units. The wind speed data used in this study are 10-meter surface wind speed data [10].

2.2.4. Solar Radiation

Solar radiation is the energy transmitted from the Sun to the Earth's surface, constituting an essential component of the Earth's energy balance. It mainly consists of electromagnetic waves, including visible light, ultraviolet (UV) radiation, and infrared (IR) radiation, and serves as a primary energy source for biological and atmospheric systems on Earth. The solar radiation data used in this study are obtained from the ERA5-LAND dataset, released by the European Centre for Medium-Range Weather Forecasts (ECMWF).

2.2.5. Vapor Pressure Deficit (VPD)

Vapor Pressure Deficit (VPD) refers to the difference in pressure between saturated water vapor and saturated water at a certain temperature. It is commonly used to describe the moisture content and saturation level of water vapor in the air.

VPD data are obtained through simulated calculations based on relative humidity, temperature, and atmospheric pressure. The calculation formula is shown as Equation (1).

$$\mathrm{VPD} = 6.11 * \exp\left(\frac{17.27 * (T - 273.15)}{T - 273.15 + 237.3}\right) - \frac{q * P}{0.622 + 0.378 * q} \quad (1)$$

In which, T represents temperature (unit: K), q represents relative humidity (a de-

cimal between 0 and 1), and P represents atmospheric pressure (unit: hPa).

2.2.6. Soil moisture

Soil moisture is a crucial parameter in land surface water and energy cycles, serving as one of the primary water sources for plant growth and photosynthesis. It plays a vital role in plant growth, soil ecosystems, hydrological cycles, and various other environmental processes.

The data used in this study are sourced from the National Tibetan Plateau Data Center [11]. The soil moisture dataset is derived using auxiliary factors such as vegetation indices (NDVI, EVI), land surface temperature (LST), evapotranspiration (ET), precipitation, terrain (DEM, slope, aspect, TWI), soil properties, and soil moisture-related indices (SWCI, SIWSI, VSDI). These factors are employed to downscale ESA CCI soil moisture data using five machine/deep learning methods: Artificial Neural Network (ANN), Convolutional Neural Network (CNN), Residual Neural Network (ResNet), Long Short-Term Memory Network (LSTM), and XGBoost. Subsequently, the downscaled soil moisture data are fused using the Bayesian three-cornered hat method to obtain the final dataset.

2.3. Statistical Analysis Methods

2.3.1. The Theil-Sen Slope Estimation Method

The Theil-Sen slope estimation is a non-parametric method used to estimate trends in time series data. It does not require assumptions about serial correlation or normal distribution in the time series. Compared to other methods, Theil-Sen slope estimation can effectively handle small outliers and missing value noise [12]. The calculation formula is shown as Equation (2).

$$\beta = \text{Median}\left(\frac{X_j - X_i}{j - i}\right), \forall j > i \tag{2}$$

In which, β represents the median slope of all data pairs. When $\beta > 0$, the data show an increasing trend; when $\beta < 0$, the data exhibit a decreasing trend. X_i and X_j are the values at time i and j in the data time series, and "Median" denotes the median value.

2.3.2. The Mann-Kendall Test Analysis Method

The Mann-Kendall (MK) test is a non-parametric trend detection method used for time series analysis, primarily aimed at assessing the significance of trends within time series data [13]. Its core purpose is to evaluate whether trends present in time series data are statistically significant. Unlike traditional parametric testing methods that rely on the assumption of normal data distribution, the advantage of the MK test lies in its lack of requirement for data distribution, while also exhibiting robustness to missing values and outliers in the data. This makes the MK test particularly suitable for analyzing and validating the significance of trends in long-term time series data. The calculation formula for the test statistic S is shown in Equation (3). In the formula for calculating Z, when S is greater than 0, the numerator is S minus 1.

$$S = \sum_{i=1}^{n-1} \sum_{j=i+1}^{n} \operatorname{sgn}\left(x_j - x_i\right) \tag{3}$$

In which, sgn() represents the sign function, and its calculation formula is shown in Equation (4).

$$\operatorname{sgn}\left(x_j - x_i\right) = \begin{cases} +1, & x_j - x_i > 0 \\ 0, & x_j - x_i = 0 \\ -1, & x_j - x_i < 0 \end{cases} \tag{4}$$

To conduct trend testing using the test statistic Z, the calculation method for the Z value is as shown in Equation (5).

$$Z = \begin{cases} \dfrac{S}{\sqrt{\operatorname{Var}(S)}}, & S > 0 \\ 0, & S = 0 \\ \dfrac{S+1}{\sqrt{\operatorname{Var}(S)}}, & S < 0 \end{cases} \tag{5}$$

In which, the calculation formula for Var is as shown in Equation (6).

$$\operatorname{Var}(S) = \frac{n(n-1)(2n+5) - \sum_{p=1}^{m} t_p\left(t_p - 1\right)\left(2t_p + 5\right)}{18} \tag{6}$$

In the equation, n represents the number of data points in the sequence; m represents the number of unique values (groupings), and t_p represents the number of repetitions for each repeated value.

The categories and characteristics of trends in the Mann-Kendall test are shown in Table 1. When the absolute value of Z exceeds 1.65, 1.96, and 2.58, it indicates that the trend passes significance tests with confidence levels of 90%, 95%, and 99%, respectively. In this study, a significance level of 95% is adopted [14].

Table 1. Table type styles (Table caption is indispensable).

β	Z	*Trend Categories*	*Trend Features*
$\beta > 0$	$2.58 < Z$	4	Extremely Significant Increase
	$1.96 < Z \leq 2.58$	3	Significant Increase
	$1.65 < Z \leq 1.96$	2	Slightly Significant Increase
	$Z \leq 1.65$	1	Not Significant Increase
$\beta = 0$	Z	0	No Change
$\beta < 0$	$Z \leq 1.65$	−1	Not Significant Decrease
	$1.65 < Z \leq 1.96$	−2	Slightly Significant Decrease
	$1.96 < Z \leq 2.58$	−3	Significant Decrease
	$2.58 < Z$	−4	Extremely Significant Decrease

2.3.3. Multiple Linear Regression Model

The multiple linear regression model is a statistical model used to explore the relationship between multiple independent variables and one continuous de-

pendent variable. In this model, the dependent variable (also known as the response variable) is assumed to be a linear combination of one or more independent variables. Each independent variable has an associated coefficient that represents the degree of its influence on the dependent variable.

$$Y = \beta_0 + \beta_1 X_1 + \beta_2 X_2 + \cdots + \beta_p X_p + \varepsilon \tag{7}$$

In which, Y is the response variable, β_0 is the intercept, β_1, β_2, $\cdots$, β_p are the coefficients of the independent variables X_1, X_2, $\cdots$, X_p; X_1, X_2, $\cdots$, X_p are the independent variables; ε is the error term, representing the part of the model that cannot be explained.

3. Results and Analysis

3.1. Spatiotemporal Variation Characteristics of GPP

The distribution of daily average GPP changes for terrestrial vegetation in the study area from 2001 to 2020 is shown in Figure 1.

Based on Figure 1, the GPP in the study area exhibits significant spatiotemporal heterogeneity. When the year is divided into four seasons—spring (March to May), summer (June to August), autumn (September to November), and winter (December to February)—the GPP values for the study area are markedly higher in summer, accounting for 60.8% of the annual GPP. Spring and autumn follow, contributing 18.91% and 13.04%, respectively. In winter, due to vegetation being nearly dormant, GPP is the lowest, accounting for only 7.19% of the annual total.

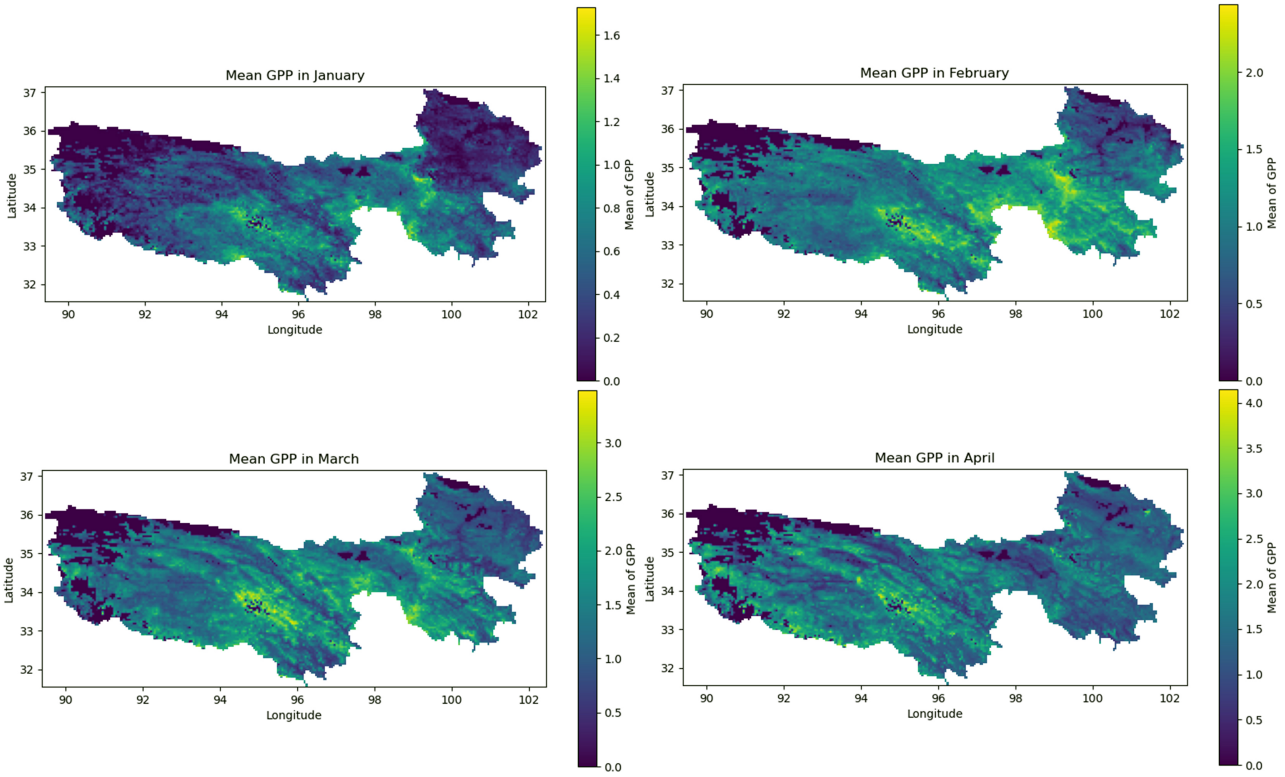

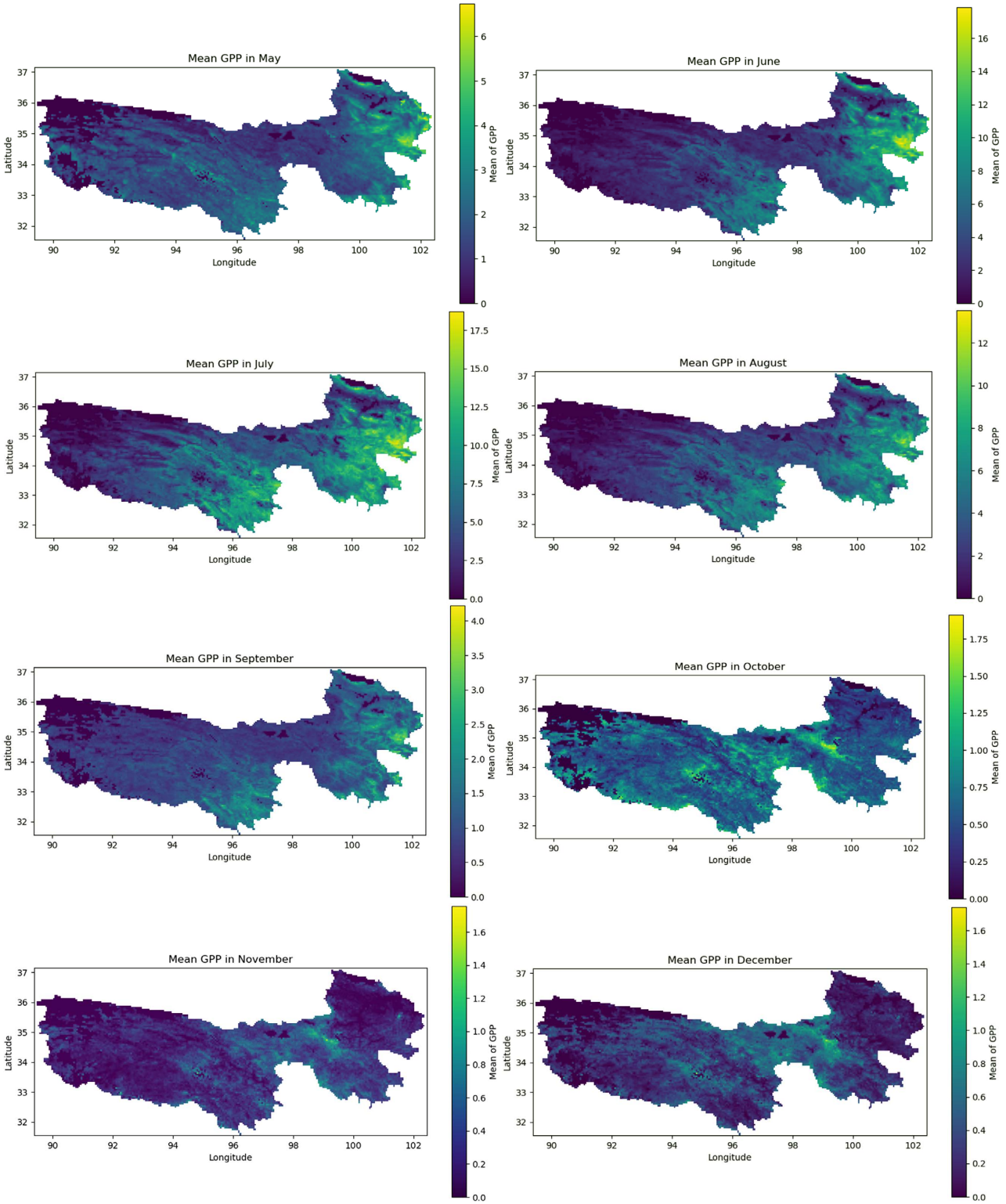

Figure 1. Distribution of daily average GPP for terrestrial vegetation in the study area from 2001 to 2020.

In terms of spatial distribution, the GPP shows a decreasing trend from southeast to northwest. The low-value areas, where the daily average GPP is below 0.5 $gC \cdot m^{-2} \cdot yr^{-1}$, are mainly located in the western part of the study area. This

region is dominated by alpine steppes, alpine desert steppes, and temperate desert steppes, with elevations mostly above 4000 meters. Regions with a daily average GPP below 0.8 $gC \cdot m^{-2} \cdot yr^{-1}$ account for 44.75% of the total area and are primarily distributed in the northern and southwestern parts of the study area. The main vegetation types in these regions are alpine meadows and alpine steppes. High-value areas, where the daily average GPP exceeds 1 $gC \cdot m^{-2} \cdot yr^{-1}$, constitute 16.67% of the total area. These regions are predominantly found in the eastern and southwestern parts of the study area and are mainly covered by alpine meadows, with some scattered shrubs and forests.

Trend analysis was conducted for each pixel in the study area, with the results shown in **Figure 2**. During the spring season, there is a clear upward trend in GPP in the northeastern part of the study area. In the summer season, apart from the central region, both the western and northeastern parts exhibit significant increases in GPP. Due to the high intensity of photosynthesis during summer, this period shows the most pronounced increase in GPP compared to the other seasons. In autumn, the trend in GPP varies significantly from summer. The northeastern part experiences a noticeable downward trend, while the central region shows a certain degree of increase, and the western region still exhibits some increase. In winter, influenced by phenological stages, photosynthesis gradually stagnates, and the GPP trend in the study area no longer shows significant spatial distribution characteristics.

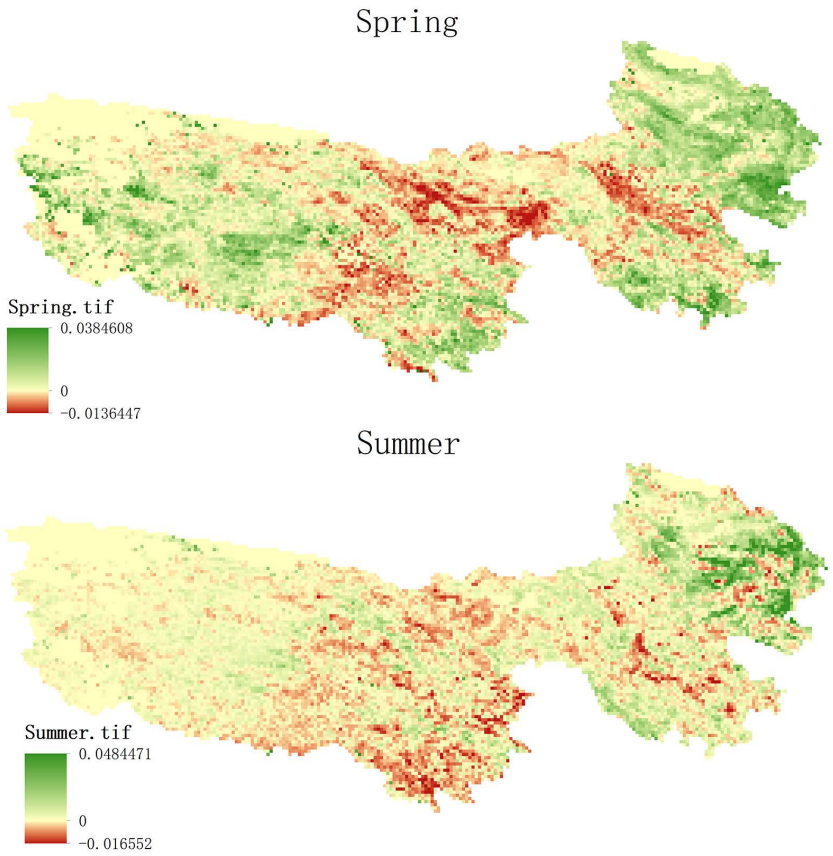

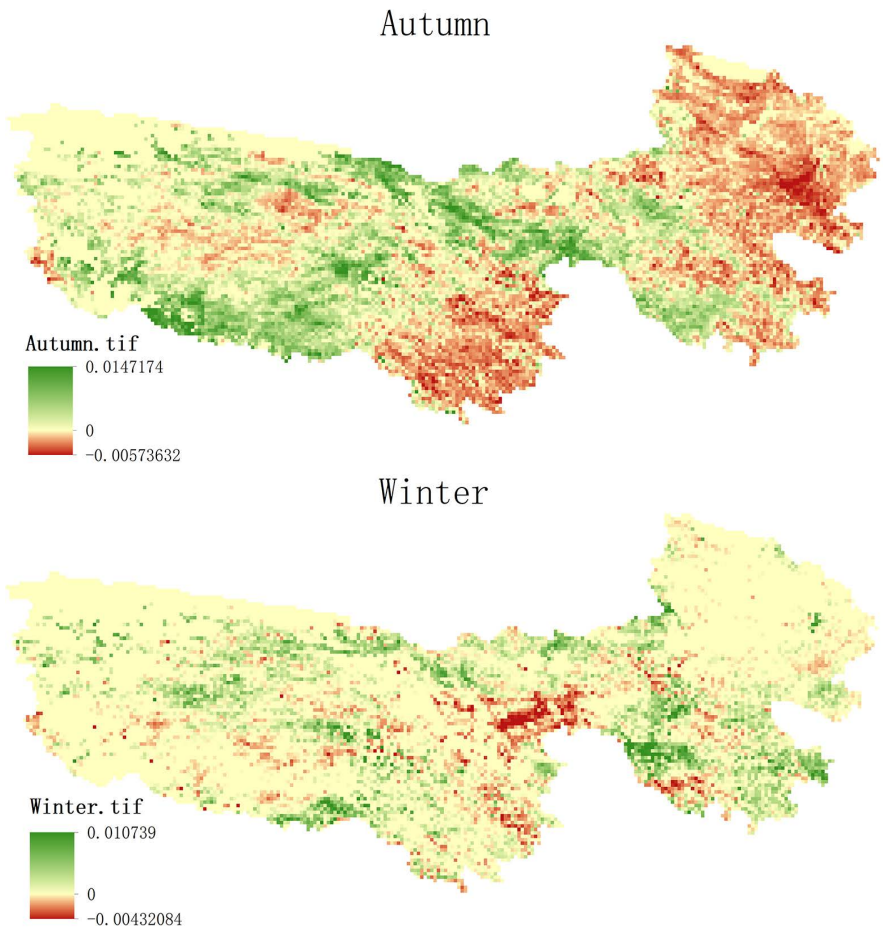

Figure 2. The spatial distribution of total GPP trends for different seasons from 2001 to 2020. In the figure, positive values indicate an increasing trend in GPP, while negative values indicate a decreasing trend in GPP.)

3.2. Establishment of the GPP Change Attribution Model

The land vegetation GPP is influenced by both the physiological characteristics of the plants themselves and external environmental factors. Among the external environmental factors, significant influences on GPP include temperature, precipitation, VPD (Vapor Pressure Deficit), soil moisture, solar radiation, and atmospheric pressure. Moisture conditions are crucial factors affecting GPP, with precipitation and soil moisture serving as indicators of moisture conditions. However, since some precipitation may be intercepted by the canopy or converted into surface runoff and may not be utilized by vegetation, and its infiltration process is influenced by soil characteristics, soil moisture can more accurately reflect the available water for vegetation than precipitation. Additionally, the VPD data used in this study are simulated based on specific humidity, air temperature, and atmospheric pressure, hence these data are not input as variables in this study.

The Leaf Area Index (LAI) is an important indicator for assessing vegetation coverage and growth status, closely related to the total primary productivity of

terrestrial vegetation. Solar radiation is the primary source of energy for photosynthesis, and its adequacy directly affects the photosynthetic rate of plants and the level of GPP. Moderate wind speed helps regulate leaf temperature and humidity, promotes gas exchange and transpiration, thereby facilitating photosynthesis. Vapor Pressure Deficit (VPD) reflects the difference in water vapor content in the atmosphere and is an important driving factor for plant transpiration. Surface temperature of land affects the physiological activities and metabolic rates of plants, while also influencing soil temperature and water evaporation rates, thus impacting the water and carbon cycles of vegetation ecosystems. Soil moisture, as one of the important water sources for plant growth, has a critical influence on plant growth and photosynthesis. Therefore, this study selects six variables: Leaf Area Index, solar radiation, wind speed, Vapor Pressure Deficit, land surface temperature, and soil moisture, to analyze the comprehensive effects of multi-factor spatial-temporal changes in GPP at the regional scale. Based on the multiple linear regression model, this paper constructs a change attribution model for regional-scale GPP, as shown in equation (8).

$$\mathrm{GPP} = a(\mathrm{LAI}) + b(\mathrm{Srad}) + c(\mathrm{Wind}) + d(\mathrm{VPD}) + e(\mathrm{T}) + f(\mathrm{SW}) + g \quad (8)$$

In which, LAI represents Leaf Area Index, Srad denotes solar radiation, Wind stands for wind speed, VPD represents Vapor Pressure Deficit, T indicates land surface temperature, SW signifies soil moisture, and a, b, c, d, e, f are fitted empirical parameters. By utilizing the established attribution model, it is possible to conduct a comprehensive analysis of the multi-factor impacts on regional-scale GPP from two dimensions: intra-annual seasonal changes and inter-annual variations. Furthermore, the contributions of the six influencing factors—LAI, LST, SVPD, Soil Moisture, Solar Radiation and Wind Speed—can be quantified in different dimensions to GPP variations.

The established GPP change attribution model was applied to simulate the intra-annual seasonal variations of GPP in the regional-scale terrestrial ecosystem of the area. The simulated values were then compared with the computational values for analysis, as illustrated in **Figure 3**.

According to **Figure 3**, the model accurately simulates the intra-annual seasonal variations of GPP at the regional scale, with 68.48% of the area showing an R^2 greater than 0.7 when compared with computational GPP. Excluding regions in the west with extremely low vegetation cover, the proportion with an R^2 greater than 0.7 increases to 77.82%, indicating that the model's simulated values are consistent with the estimated GPP. Therefore, for the overall study area, the GPP change attribution analysis model can effectively explain the intra-annual seasonal variations of regional-scale GPP.

3.3. Analysis of Driving Factors for GPP Variations

Quantification of the Relative Contributions of LAI, LST, SVPD, Soil Moisture, Solar Radiation and Wind Speed to the Seasonal Variations of Regional-Scale GPP Based on the GPP Variation Attribution Analysis Model.

3.3.1. Analysis of Driving Factors for Spring GPP Variations

The spatial distribution of the relative contributions of different driving factors to the changes in GPP during spring can be seen in Figure 4.

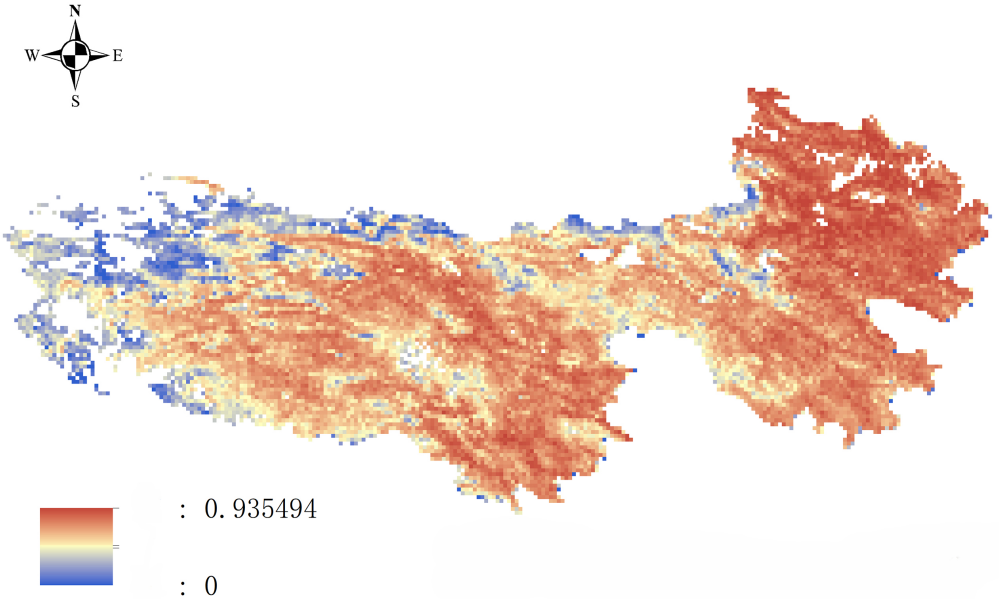

Figure 3. The distribution of the correlation coefficient R2 between the simulated GPP by model and the computational GPP (The goodness of fit for the model, R^2, can reach up to 0.935494).

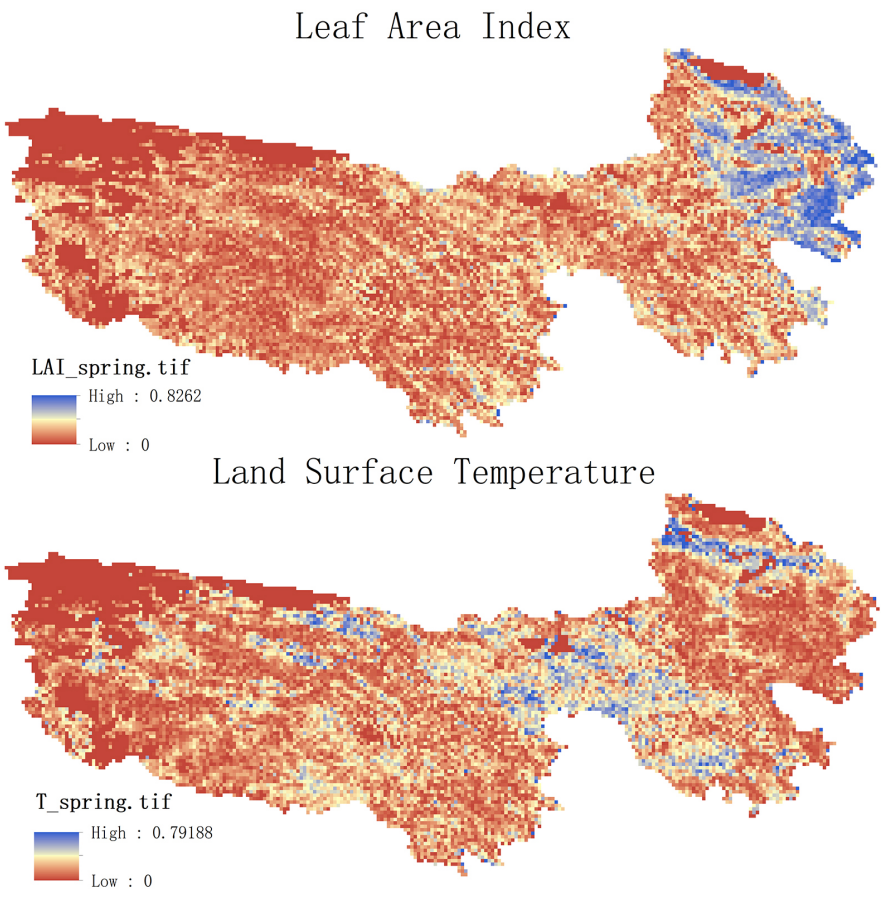

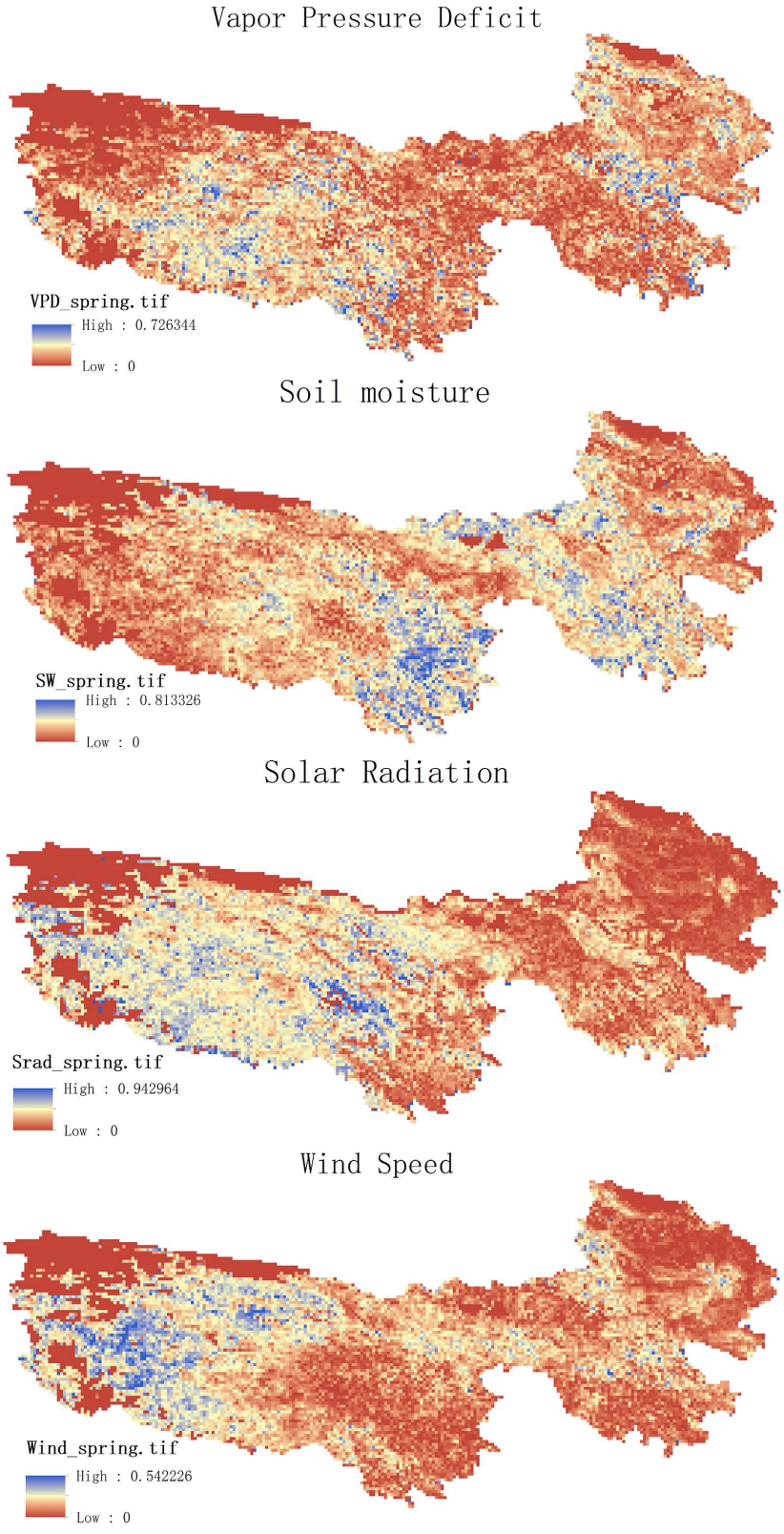

Figure 4. Spatial distribution of the relative contributions of different driving factors to spring GPP variations. (In the figure, "High" indicates the highest contribution ratio of the influencing factor to GPP, while "Low" indicates the lowest contribution ratio of the influencing factor to GPP).

According to Figure 4, in the spring season (March to May), the contribution of LAI to GPP shows a higher degree in the eastern region compared to the western region. This may be attributed to the more suitable soil types and moisture conditions in the eastern region, promoting rapid vegetation growth during spring. Consequently, the vegetation cover is denser in the east, leading to a relatively higher contribution of LAI to GPP. The contributions of Solar Radiation and Wind Speed, on the other hand, exhibit higher values in the western region and lower values in the east. The western areas, being more open and less obstructed by mountainous terrain, receive ample sunlight during spring, while higher wind speeds facilitate gas exchange and transpiration in vegetation, thus contributing more significantly to GPP. Soil Moisture, on the other hand, shows higher contributions in the southern region and lower contributions in surrounding areas. The southern region likely experiences higher precipitation during spring, resulting in relatively abundant soil moisture, which enhances vegetation growth and contributes more significantly to GPP. VPD and LST exhibit generally lower contributions, possibly due to lower temperatures and higher humidity during spring, leading to reduced sensitivity of vegetation to these factors and thus lower contributions to GPP.

3.3.2. Analysis of Driving Factors for Summer GPP Variations

The spatial distribution of the relative contributions of different driving factors to the changes in GPP during summer can be seen in Figure 5.

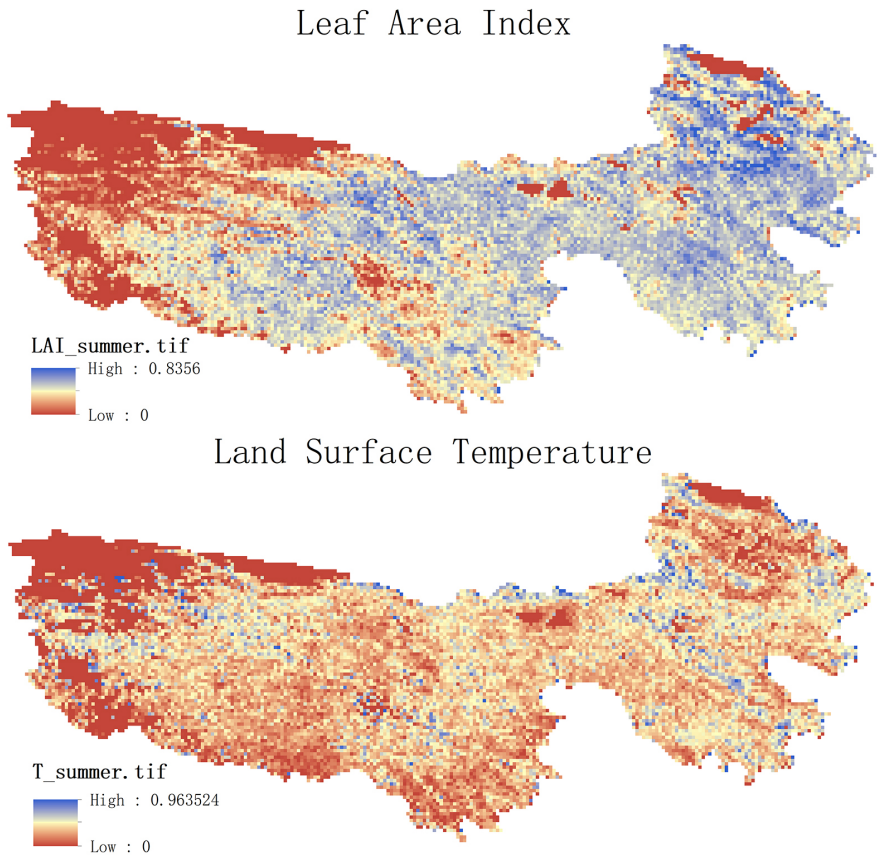

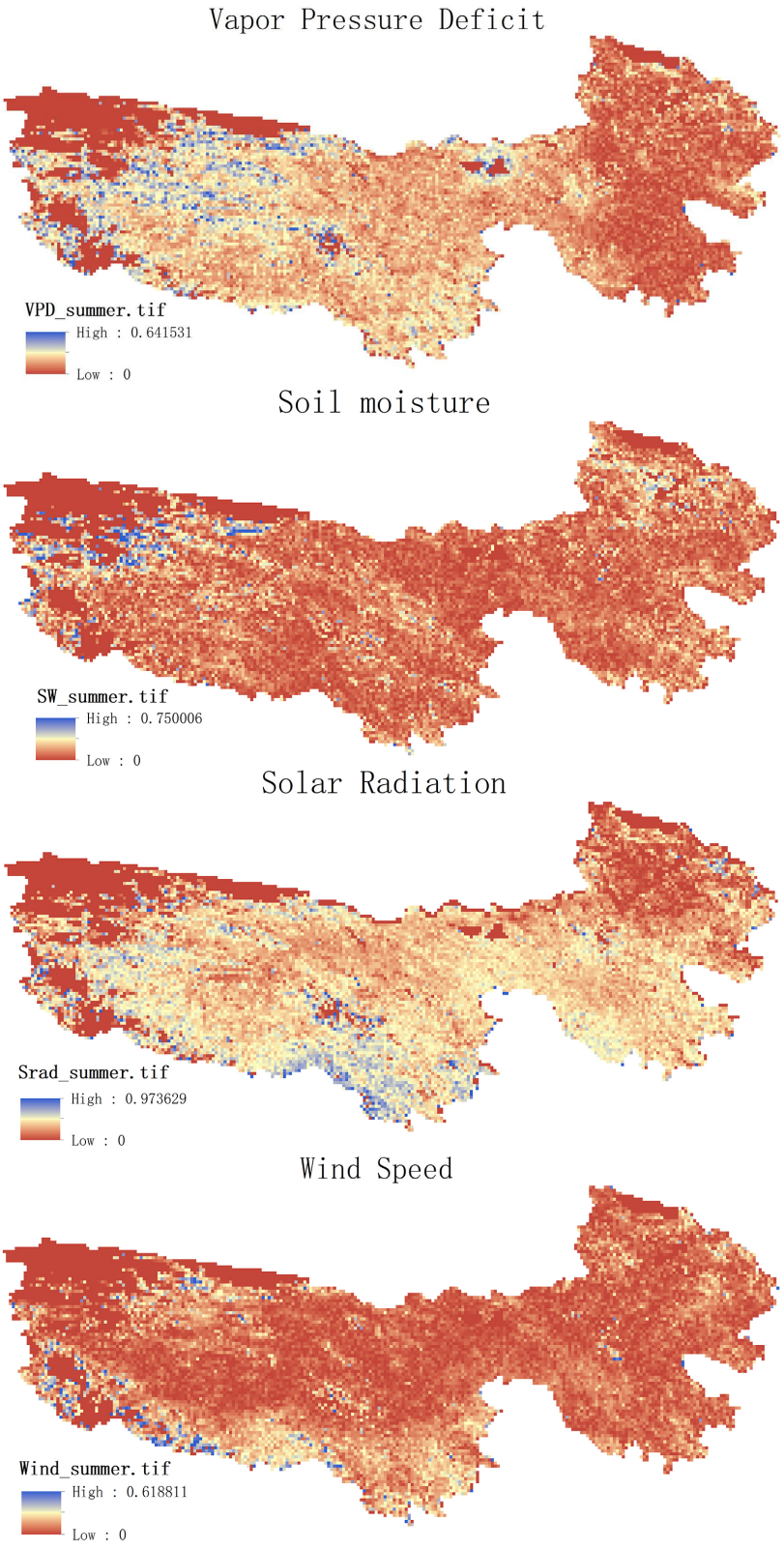

Figure 5. Spatial distribution of the relative contributions of different driving factors to summer GPP variations. (In the figure, "High" indicates the highest contribution ratio of the influencing factor to GPP, while "Low" indicates the lowest contribution ratio of the influencing factor to GPP.)

According to Figure 5, in the summer months (June-July), the contribution of LAI and GPP shows a gradual increase from west to east. Compared to spring, there is a significant increase in contribution in the central region, which may be due to the presence of more precipitation resources and favorable climatic conditions in the eastern region, promoting vegetation growth and coverage. In contrast, the western region, due to its rugged terrain and higher altitudes, experiences harsher climatic conditions and relatively weaker vegetation growth. This leads to higher contribution of LAI in the eastern region, while in the central region, the contribution significantly increases due to more favorable climatic conditions. There is no clear spatial distribution observed for LST, Wind Speed, and Soil Moisture in terms of their contributions to GPP. This may be because there are no significant temperature gradients and wind speed differences in summer, resulting in no apparent spatial variations in their effects on GPP. With relatively abundant summer precipitation, soil moisture remains relatively adequate across the region, showing no significant differences in its relative contribution to GPP. Solar radiation exhibits a gradual decrease from south to north, possibly due to the higher latitude in the northern region resulting in a smaller solar zenith angle and consequently lower received solar radiation. Conversely, in the southern region, where the solar zenith angle is larger, solar radiation is relatively higher.

3.3.3. Analysis of Driving Factors for Autumn GPP Variations

The spatial distribution of the relative contributions of different driving factors to the changes in GPP during autumn can be seen in Figure 6.

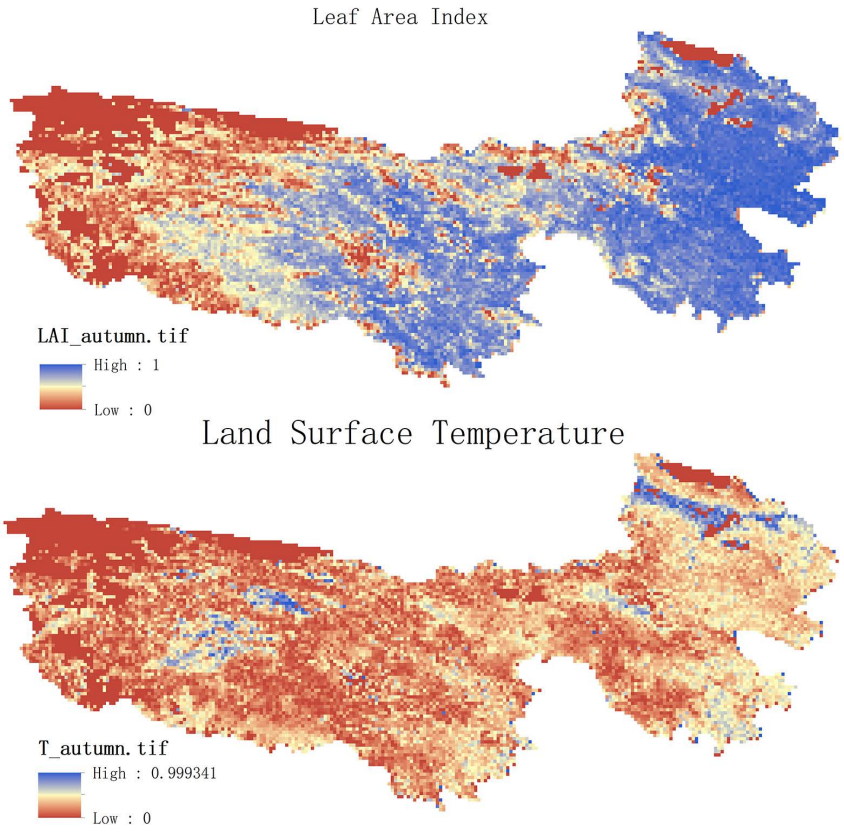

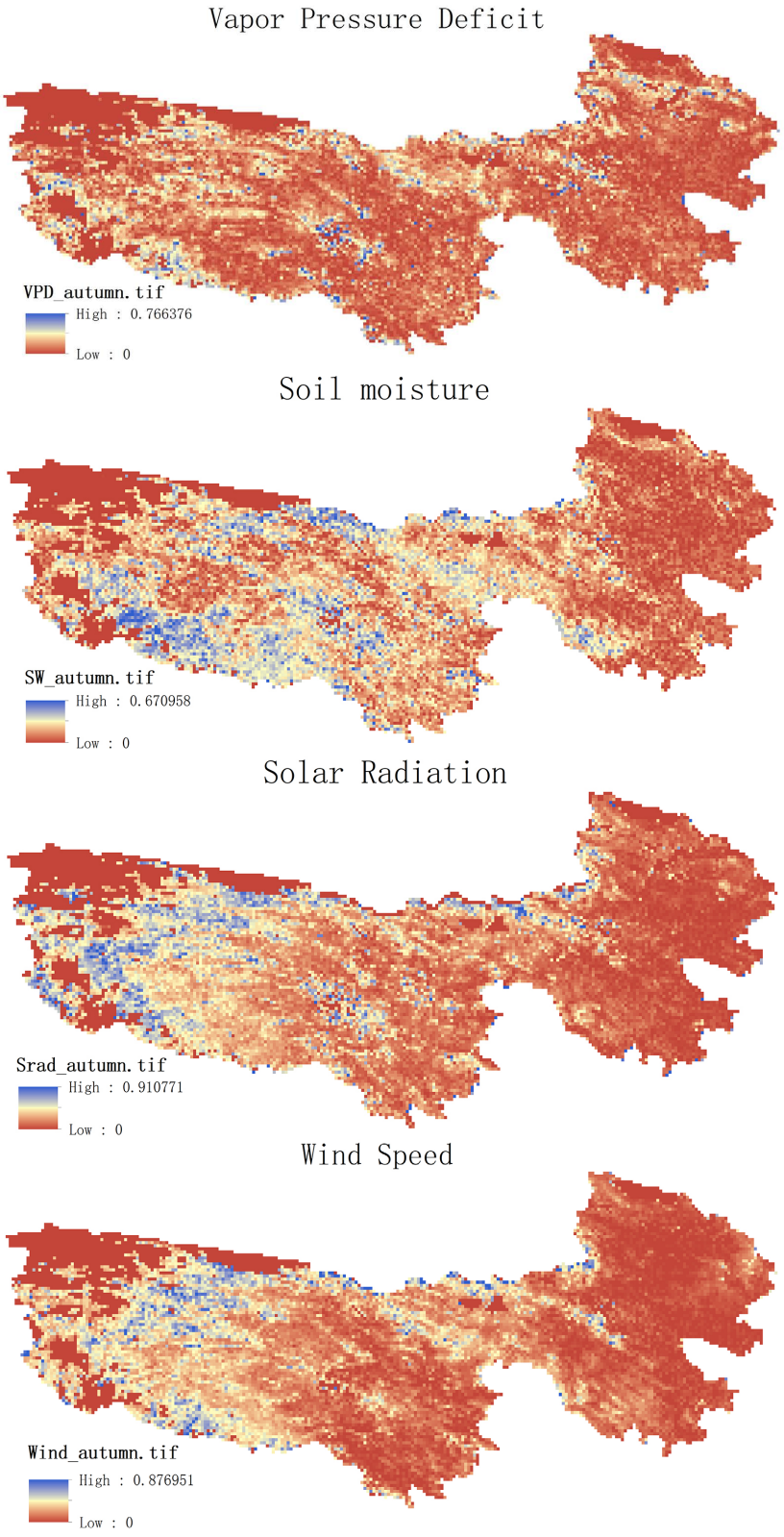

Figure 6. Spatial distribution of the relative contributions of different driving factors to autumn GPP variations. (In the figure, "High" indicates the highest contribution ratio of the influencing factor to GPP, while "Low" indicates the lowest contribution ratio of the influencing factor to GPP.)

According to Figure 6, in the autumn months (August-November), LAI shows high relative contributions to GPP across the entire region, except for the western region where the correlation is relatively low. This could be attributed to factors such as terrain, soil type, or vegetation type in the western region, which may limit vegetation growth and variations in land surface temperature. The spatial distribution of LST in relation to its relative contribution to GPP is similar to that of LAI. However, the spatial distribution of Soil Moisture, VPD, Solar Radiation, and Wind Speed in relation to their relative contributions to GPP is opposite to that of LAI and LST. This could be because the influences of LAI and land surface temperature on GPP are too prominent, overshadowing the effects of other factors, resulting in relatively smaller contributions from these factors.

3.3.4. Analysis of Driving Factors for Winter GPP Variations

The spatial distribution of the relative contributions of different driving factors to the changes in GPP during winter can be seen in Figure 7.

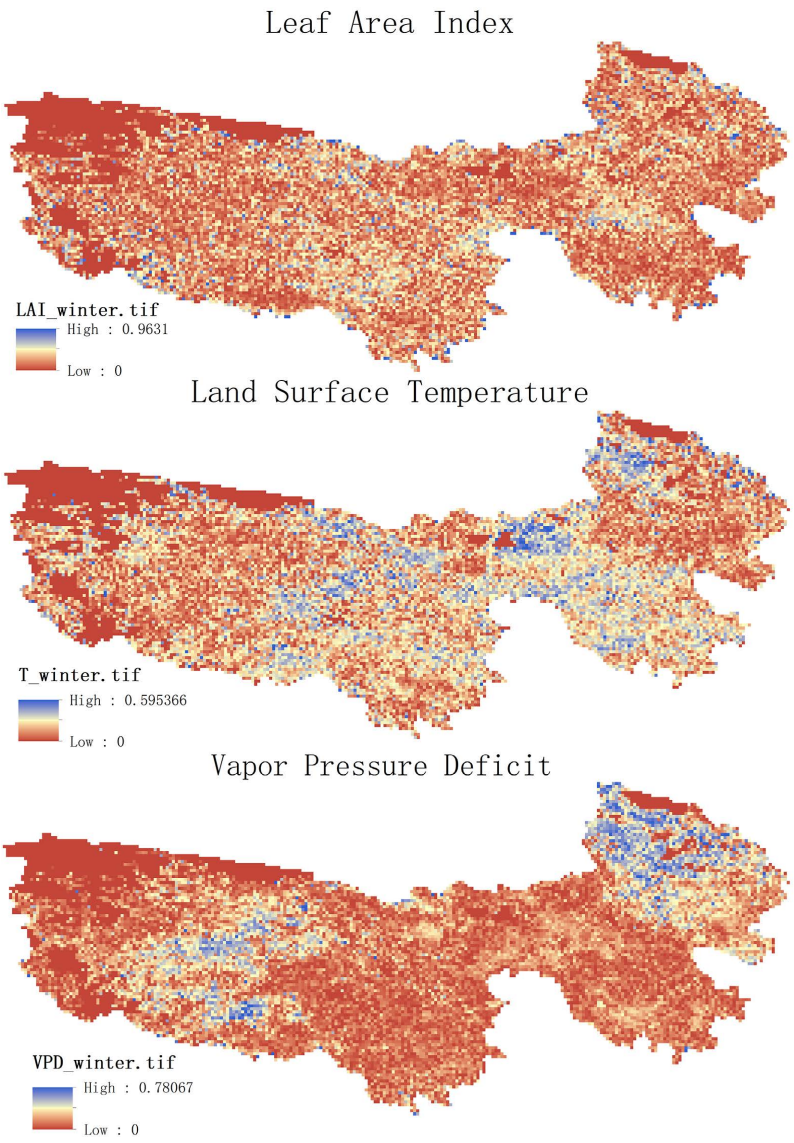

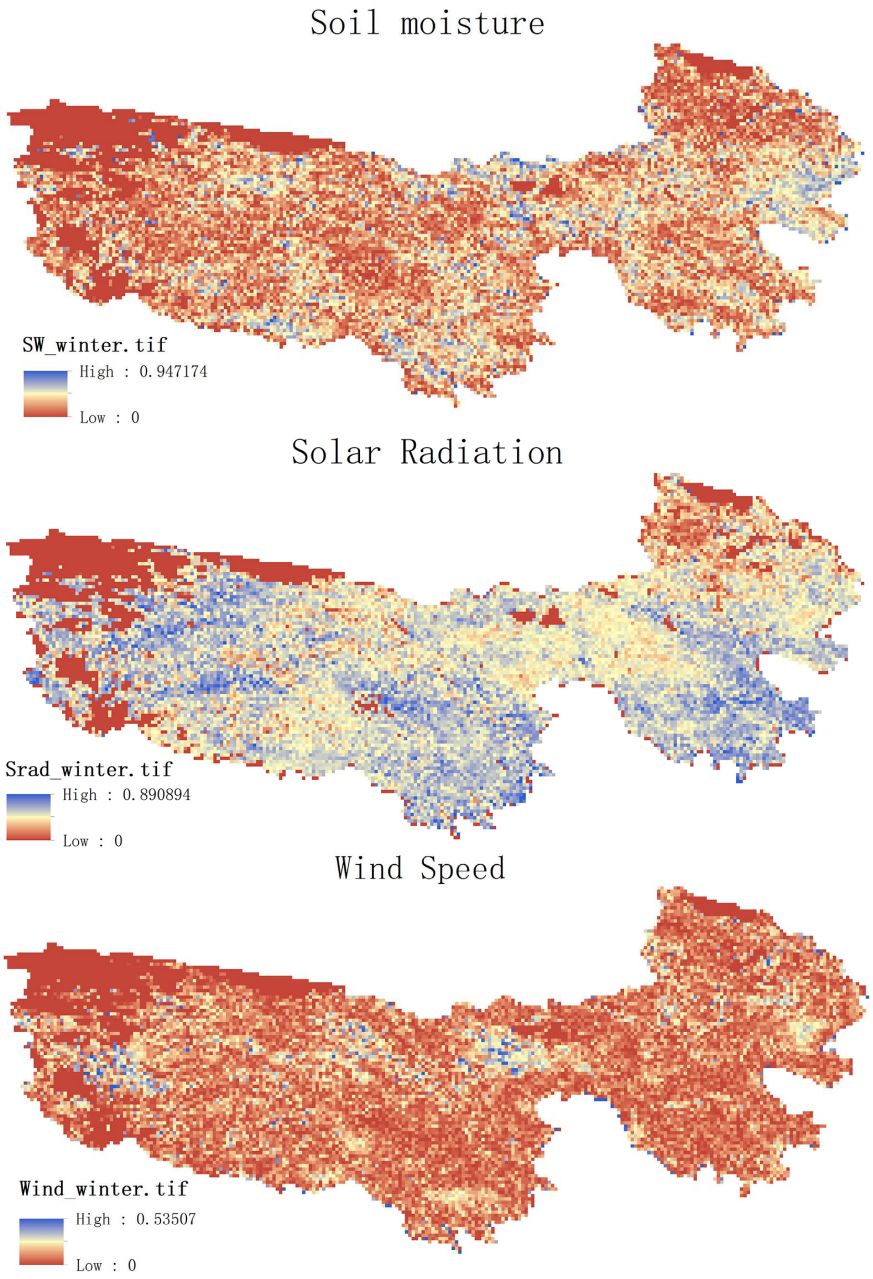

Figure 7. Spatial distribution of the relative contributions of different driving factors to winter GPP variations. (In the figure, "High" indicates the highest contribution ratio of the influencing factor to GPP, while "Low" indicates the lowest contri-bution ratio of the influencing factor to GPP.)

According to **Figure 7**, in the winter months (December-February), LAI, LST, and Wind Speed show no distinct spatial distribution characteristics regarding their relative contributions to GPP across entire study region. Three-River Source Region. Overall, they exhibit lower correlations with GPP, as winter is a season when vegetation growth activities slow down, resulting in lower vegetation coverage and hence lower contributions from LAI to GPP. The generally low temperatures in winter also slow down plant growth activities, leading to

lower overall correlations between land surface temperature and GPP. Soil Moisture exhibits higher relative contributions in the central part of the study area, while lower contributions are observed in the surrounding areas. Conversely, VPD shows the opposite trend, with higher relative contributions in the eastern and western regions and lower contributions in the central region. This may be related to the topographic and hydrological features of the area. The central region may contain lakes, rivers, and other water bodies, which could accumulate a significant amount of water during winter, resulting in relatively abundant soil moisture in the surrounding areas. The presence of these water bodies can provide sufficient water sources, promoting soil moisture and vegetation growth, and consequently increasing GPP. Higher soil moisture may lead to relatively higher humidity levels in the surrounding air, resulting in lower VPD. Conversely, the eastern and western regions may have relatively less soil moisture, leading to higher air dryness and hence higher VPD. Despite the shorter duration of sunlight in winter, Solar Radiation shows a significantly increased contribution to GPP. This could be due to the adequacy of solar radiation in winter and the relatively lower photosynthetic rates of vegetation during this season.

4. Conclusions

This study systematically analyzed the spatiotemporal variation characteristics of land vegetation GPP and its driving factors based on Sun-Induced Chlorophyll Fluorescence (SIF) remote sensing data estimation. It quantified the relative contributions of each driving factor to GPP changes, providing a basis for a deeper understanding of the driving mechanisms of regional-scale GPP variations.

1) The land vegetation GPP in the study area exhibits significant spatiotemporal variations.

In spring, with the rise in temperature and increasing daylight hours, vegetation enters the growing season, leading to a rapid increase in GPP as the phenological stages of bud burst and heading occur.

Summer marks the peak growing season for vegetation in the study area, characterized by high temperatures and humidity, facilitating lush vegetation growth and resulting in the highest GPP levels of the year. Vegetation phenology exhibits vigorous growth characteristics during this period.

As autumn approaches, temperatures gradually decrease, and daylight hours shorten, leading vegetation to enter the senescence stage. GPP begins to decline as vegetation transitions into the withering and leaf shedding period.

Winter represents the dormant season in the study area, marked by a sharp drop in temperature and vegetation entering a dormant state. GPP significantly decreases during this period, and vegetation phenology reflects a dormant phase.

Apart from seasonal variations, vegetation phenology in the study area is also influenced by geographical location and altitude. In lower altitude areas, vegeta-

tion phenology occurs relatively earlier, with longer growing seasons and higher GPP. Conversely, in higher altitude areas, vegetation phenology occurs later, with shorter growing seasons and lower GPP. This spatiotemporal variation reflects the adaptive capacity of vegetation to climate and topography in the study area, as well as the vulnerability and sensitivity of high-altitude cold regions' vegetation ecosystems.

2) The regional-scale GPP attribution analysis model was constructed, with 68.48% of the area's simulated results showing an R-squared value greater than 0.7 compared to the estimated GPP. Excluding regions in the west with extremely low vegetation cover, 77.82% of the area's simulated results show an R-squared value greater than 0.7 compared to the computational GPP.

3) LAI dominates both the spatial and seasonal variations of regional-scale GPP, with GPP increasing as LAI increases. On the other hand, variables like VPD , LST, Solar Radiation, and Soil Moisture have varying effects on GPP across different dimensions. Additionally, wind speed shows relatively smaller contributions to GPP across different dimensions.

Conflicts of Interest

The author declares no conflicts of interest regarding the publication of this paper.

References

[1] Forzieri, G., Alkama, R., Miralles, D.G., *et al.* (2017) Satellites Reveal Contrasting Responses of Regional Climate to the Widespread Greening of Earth. *Science* (*American Association for the Advancement of Science*), **356**, 1180-1184. https://doi.org/10.1126/science.aal1727

[2] Melillo, J.M., McGuire, A.D., Kicklighter, D.W., *et al.* (1993) Global Climate Change and Terrestrial Net Primary Production. *Nature*, **363**, 234-240. https://doi.org/10.1038/363234a0

[3] Diffenbaugh, N.S. and Burke, M. (2019) Global Warming Has Increased Global Economic Inequality. *Proceedings of the National Academy of Sciences*, **116**, 9808-9813. https://doi.org/10.1073/pnas.1816020116

[4] Li, X., Liang, S., Yu, G., *et al.* (2013) Estimation of Gross Primary Production over the Terrestrial Ecosystems in China. *Ecological Modelling*, **261-262**, 80-92. https://doi.org/10.1016/j.ecolmodel.2013.03.024

[5] Zhou, S. (2017) Study on the Potential Water Use Efficiency Model of Terrestrial Ecosystems and Its Application. Ph.D. Thesis, Tsinghua University. (In Chinese)

[6] Zhu, X., Zhang, S., Liu, T., *et al.* (2021) Impacts of Heat and Drought on Gross Primary Productivity in China. *Remote Sensing*, **13**, Article 378. https://doi.org/10.3390/rs13030378

[7] Beer, C., *et al.* (2010) Terrestrial Gross Carbon Dioxide Uptake: Global Distribution and Covariation with Climate. *Science*, **329**, 834-838. https://doi.org/10.1126/science.1184984

[8] Xia, Z. (2024) The Spatiotemporal Variation of Terrestrial Vegetation Phenology and Its Driving Factors in the Sanjiangyuan Region. Master's Thesis, Qinghai University. (In Chinese)

[9] Zhang, X.D., Ding, L.R., Zhou, J., *et al*. (2023) Daily 1km All-Weather Land Surface Temperature Dataset for China's Land and Surrounding Areas (TRIMS LST; 2000-2022). National Tibetan Plateau Data Center. National Tibetan Plateau Data Center. https://doi.org/10.11888/Meteoro.tpdc.271252

[10] Shao, C.K., Jiang, Y.Z., Yang, K., *et al*. (2023) Long-Term High-Resolution Ground Meteorological Forcing Dataset for the Third Pole Region (TPMFD, 1979-2022). National Tibetan Plateau Data Center. National Tibetan Plateau Data Center. https://doi.org/10.11888/Atmos.tpdc.300398

[11] Shangguan, Y.L., Shi, Z. and Min, X.X. (2023) Daily 1km Soil Moisture Dataset of the Tibetan Plateau (2001-2020). National Tibetan Plateau Data Center. National Tibetan Plateau Data Center. https://doi.org/10.11888/Terre.tpdc.300224

[12] Gu, C.J., Zhang, Y.L., Liu, L.S., *et al*. (2023) Consistency Assessment of Four NDVI Datasets in the Sanjiangyuan Region of Qinghai. *Geographical Research*, **42**, 1378-1392.

[13] Liu, C. (2022) Study on the Impact of Vegetation Restoration on Soil Moisture in the Loess Plateau. Master's Thesis, Hebei GEO University.

[14] Tian, Z.H., Ren, Z.G. and Wei, H.T. (2022) Driving Mechanisms of Vegetation Spatiotemporal Evolution in the Yellow River Basin from 2000 to 2020. *Environmental Science*, **43**, 743-751. https://doi.org/10.13227/j.hjkx.202105213